Testing the Accuracy of Machine Learning-Based Crack Localization Methods using Damage Localization Coefficients

Gilbert-Rainer GILLICH
Department of Engineering Science, Babeş-Bolyai University, Cluj-Napoca, Romania, gilbert.gillich@ubbcluj.ro

Vasile Catalin RUSU
Department of Computer Science, Babeş-Bolyai University, Cluj-Napoca, Romania, vasile.rusu@ubbcluj.ro

Cristian TUFISI*
Department of Engineering Science, Babeş-Bolyai University, Cluj-Napoca, Romania, cristian.tufisi@ubbcluj.ro

Nicoleta GILLICH
Department of Engineering Science, Babeş-Bolyai University, Cluj-Napoca, Romania, nicoleta.gillich@ubbcluj.ro

Cosmina IONUT
Department of Computer Science, Babeş-Bolyai University, Cluj-Napoca, Romania, cosmina.ionut@stud.ubbcluj.ro

Abstract: - Artificial intelligence is often used to assess the integrity of engineering structures. Many methods are available to assess different types of damage, but the correctness of the results is not proven until local inspection methods are applied. Therefore, there is a need to develop a tool that can estimate the accuracy of the assessment process through a supplementary intervention. In this paper, we propose and test a procedure to establish the accuracy of the damage assessment results, which is the follow-up of a normal damage assessment process. First, we assess the damage involving a method previously developed by the authors that consider the relative frequency shifts (RFS) for several bending vibration modes. The method has the support of artificial neural networks (ANN). Applying this method, we estimate the location and severity of the damage. Next, we apply a procedure that presumes first to calculate the modal curvatures and the resulting damage location coefficients (DLC) for this location. Then, we normalize the RFSs used in the assessment process and compare them with the DLCs derived analytically for the presumed damage location. Finally, we compare the DLCs with the normalized RFSs via the Euclidian distance. This comparison shows how accurately we assessed the damage location, the smaller the distance, the better the prediction. Applying this procedure as a follow-up of a standard damage detection process, we know the accuracy of the assessment prediction realized with a standard detection method. If the accuracy is unsatisfactory, we can use an ANN model that is trained with data from the supposedly defective area.

Keywords: - Beam, Damage detection, natural frequencies, Machine learning, Damage location coefficients

1. INTRODUCTION

Detecting damage like cracks based on the analysis of vibration signals involves the association of changes in the modal parameters with the position and depth of the defect [1]. Currently, there are many methods for detecting defects, most based on analyzing natural frequency changes [2-5] since these are easy to be measured in real-world applications. Some methods involve changes in mode shapes [6-9] or modal curvatures [10-13].

Classically, the comparison between the response of the structure and that of the model is made using various metrics [14]. In the last decades, more and more methods have used artificial intelligence to determine the characteristics of cracks [15-20]. More recently, some of these methods process images to establish the existence and extension of cracks, but they cannot estimate the depth of the defect [21]. The latter methods can also not detect delamination or other damage located inside the structure.

In previous works, we presented a way of locating and estimating the severity of the defect [22,23] based on an artificial neural network (ANN). The accuracy is satisfactory in most cases, but there is no indication of possible errors in locating the damage.

In this paper, we introduce a procedure to evaluate the accuracy of the crack location obtained with a standard vibration-based damage detection method. In our example, we use a method that an ANN model supports, but it can estimate the accuracy of location prediction made with any damage detection method. The procedure allows us to interpret the result and possibly correct the estimated crack position. Using this procedure, we gain credibility for the estimates made, or if a significant error results, the operator is aware that another method of detecting the defect must be applied.

2. THE MACHINE-LEARNING-BASED CRACK DETECTION METHOD

The crack detection method that the Babeș-Bolyai University research group has developed is based on the relative frequency shift (RFS). This feature represents the difference between the frequency of the intact beam and that of the structure with a crack f_{iD}, normalized with f_{iU}, as proposed in [24]:

$$\Delta\bar{f}_i = \frac{f_{iU} - f_{iD}}{f_{iU}} \tag{1}$$

In equation (1), the index i represents the mode number of the out-of-plain vibration, and indices U and D indicate the undamaged and damaged state, respectively.

The equation to calculate the frequency of the beam with one transverse crack [25], situated at location x and having the depth a, is:

$$f_{iD} = f_{iU}\left\{1 - \gamma(a)\left[\bar{\phi}_i''(x)\right]^2\right\} \tag{2}$$

In this equation, $\gamma(a)$ is the severity of the crack with depth a, and $\bar{\phi}_i''(x)$ is the normalized modal curvature calculated at location x for the vibration mode i. The relation of the modal curvature for beams with various support types is well-known. The severity may be calculated using relations found from experiments (fracture mechanics method) [26, 27] or from the energy loss reflected in an increased deflection [28]. In the latter case, it is:

$$\gamma(a) = \frac{\sqrt{\delta_D(a)} - \sqrt{\delta_U}}{\sqrt{\delta_D(a)}} \tag{3}$$

In equation (3), $\delta_D(a)$ is the deflection of the free end of a cantilever beam with the crack of depth a at the fixed end, and δ_U is the deflection of the beam without a crack. The relative frequency shift is calculated for frequencies determined analytically, with the help of the finite element method (FEM), or for experimental results. For the first case, replacing equation (2) in equation (1), we obtain:

$$\Delta\bar{f}_i = \gamma(a)\left[\bar{\phi}_i''(x)\right]^2 \tag{4}$$

We calculate the RFSs with equation (1) for the measured and simulated data.

With equation (4), we can generate training data for the ANN. We calculate the RFSs for the crack parameters x and a; these are the output data. Usually, we consider eight vibration modes, which can be excited in a controlled manner and for which we obtain relevant acceleration amplitudes. The set of RFSs is the input data. We present an example of input and target data in Table 1.

Table 1. Example of Input and Target Data.

Input				***Target***	
RFS₁ [Hz/Hz]	***RFS₂*** [Hz/Hz]	***RFS₃*** [Hz/Hz]	***RFS₄*** [Hz/Hz]	***x*** [m]	***a*** [mm]
0.002901	0.001938	0.001239	0.000688	0.05	0.8
0.000612	0.000174	0.000011	0.000032	0.116	0.5
0.000673	0.001240	0.000631	0.000516	0,420	1
0.000013	0.000333	0.001481	0.002704	0.830	1.2
0.001809	0.003739	0.001460	0.001968	0.430	1.6

To train the network, we generate data for 501 positions of the crack along the beam. We consider eight crack depths for each position, resulting in 4008 damage scenarios. To save space, we show in Table 1 the RFS values for just four weak-axis bending vibration modes. However, we use eight values in this study, as mentioned earlier. The data in Table 1 is obtained from calculus, and the comparison will be made for damage detection on real-world structures, which implies measured data. Thus, the necessity of estimating the frequencies with high precision. To estimate the natural frequencies very accurately, we developed special excitation methods [30] and signal-processing algorithms [31] that have proven robust and reliable. Since they base on interpolation, these algorithms permit obtaining the frequencies on inter-line positions of the spectrum.

The hyper-parameters of the feedforward ANN model are presented in Table 2.

Table 2. Hyper-parameters of the ANN model.

Hyper-parameter	Value	
no of input and output neurons	8	2
no. of hidden layers	3	
no. of hidden layer neurons	30/layer	
activation function	tanh	
training function	Levenberg Marquardt	
training epochs	1000	
samples used for training	70%	
samples used for validation	15%	
samples used for testing	15%	

The ANN was used was developed using 70% of the data for training and 15% for testing. The rest of the 15% of the data is for validation. The ANN can depict the depth and position of cracks even for damage scenarios that do not belong to the training set. It is worth mentioning that by using equations (1) to (3), we can develop a database for any boundary conditions of the beam if the proper relationship for the mode shape is used.

3. PROCEDURE TO ESTIMATE THE LOCALIZATION ACCURACY

One feature of the RFS is that it contains information about the crack's location and severity. The effect of the crack location is associated with the vibration mode number; see the term $\overline{\phi}_i''(x)$ in equation (4). Differently, the effect of crack depth is the same regardless of the mode number. This feature allows us to remove the severity from the RFS by normalizing all RFSs for one location with the biggest in the series.

This means that after normalization, for a given crack depth a, instead of the RFS, we obtain the damage location coefficient (DLC). The mathematical relation to calculate the DLC is [29]:

$$\Phi_1 = \frac{\Delta\overline{f}_1}{\max\left\{\Delta\overline{f}_i\right\}} = \frac{\gamma(a)\left[\overline{\phi}_1''(x)\right]^2}{\max\left\{\gamma(a)\left[\overline{\phi}_i''(x)\right]^2\right\}} = \frac{\left[\overline{\phi}_1''(x)\right]^2}{\max\left\{\left[\overline{\phi}_i''(x)\right]^2\right\}} \qquad \Phi_1 = \frac{\left[\overline{\phi}_1''(x)\right]^2}{\max\left\{\left[\overline{\phi}_i''(x)\right]^2\right\}}$$

$$\Phi_2 = \frac{\Delta\overline{f}_2}{\max\left\{\Delta\overline{f}_i\right\}} = \frac{\gamma(a)\left[\overline{\phi}_2''(x)\right]^2}{\max\left\{\gamma(a)\left[\overline{\phi}_i''(x)\right]^2\right\}} = \frac{\left[\overline{\phi}_2''(x)\right]^2}{\max\left\{\left[\overline{\phi}_i''(x)\right]^2\right\}} \quad \text{or} \quad \Phi_2 = \frac{\left[\overline{\phi}_2''(x)\right]^2}{\max\left\{\left[\overline{\phi}_i''(x)\right]^2\right\}} \tag{5}$$

... ...

$$\Phi_8 = \frac{\Delta\overline{f}_8}{\max\left\{\Delta\overline{f}_i\right\}} = \frac{\gamma(a)\left[\overline{\phi}_8''(x)\right]^2}{\max\left\{\gamma(a)\left[\overline{\phi}_i''(x)\right]^2\right\}} = \frac{\left[\overline{\phi}_8''(x)\right]^2}{\max\left\{\left[\overline{\phi}_i''(x)\right]^2\right\}} \qquad \Phi_8 = \frac{\left[\overline{\phi}_8''(x)\right]^2}{\max\left\{\left[\overline{\phi}_i''(x)\right]^2\right\}}$$

Because of normalization, the DLCs for a given scenario are numbers between 0 and 1. Knowing the crack location estimated with the ANN, we can easily find the DLCs for that location. Similarly to the calculated DLCs, we can find the normalized relative frequency shifts, which are the equivalent of the DLCs for the measured or simulated data. We use equation (1) to find the DLCs in this case. It results in the series shown in equation (6).

The DLCs in equation (6) are also values between 0 and 1. If the location was estimated with error zero, the series Φ:{Φ_1 … Φ_8} and F:{F_1 … F_8} are identical. A slight difference between the two series is possible due to errors in the measured data. If more substancial differences occur, the crack's location is not estimated accurately enough. The more significant the difference, the bigger the estimation error.

$$F_1 = \frac{\Delta\overline{f}_1}{\max\left\{\Delta\overline{f}_i\right\}} = \frac{\dfrac{f_{1U} - f_{1D}}{f_{1U}}}{\max\left\{\dfrac{f_{iU} - f_{iD}}{f_{iU}}\right\}}$$

$$F_2 = \frac{\Delta\overline{f}_2}{\max\left\{\Delta\overline{f}_i\right\}} = \frac{\dfrac{f_{2U} - f_{2D}}{f_{2U}}}{\max\left\{\dfrac{f_{iU} - f_{iD}}{f_{iU}}\right\}} \tag{6}$$

...

$$F_8 = \frac{\Delta\overline{f}_8}{\max\left\{\Delta\overline{f}_i\right\}} = \frac{\dfrac{f_{8U} - f_{8D}}{f_{8U}}}{\max\left\{\dfrac{f_{iU} - f_{iD}}{f_{iU}}\right\}}$$

The comparison is possible using different metrics. In this study, we use the Euclidian distance. We calculate the distance using the mathematical relation:

$$d_{\varepsilon} = \sqrt{\sum_{i=1}^{8} \left(\Phi_i - F_i\right)^2} \quad (7)$$

Hence, the dimension of d_{ε} reflects qualitatively the error in estimating the crack location. To find this location more accurately, one should compare neighbor DLCs with the measured one and check for a better fit.

4. GENERATING DATA FOR VALIDATION

We conducted simulations in ANSYS by creating several damage scenarios for testing the ANN. The cantilever beam model was created with similar dimensions and boundary conditions, as described in the paper [22]: length L=1 m, width w=50 mm, and thickness h=5 mm. The Structural Steel material is assigned from the ANSYS library. The simulations were set up to determine the first eight natural frequencies associated with the transverse vibration modes of the beam. Six damage scenarios were generated by introducing breathing cracks at different depths and locations. The simulation involved utilizing the extrude cut feature in ANSYS for generating the crack geometry.

The crack depths varied across the scenarios, ranging from 0.4 mm to 1.6 mm. We obtained the natural frequencies of the undamaged and damaged beam models through the modal analysis. These frequencies served us to calculate the RFSs, which quantified the deviation caused by the damage.

5. RESULTS AND DISCUSSION

To prove the concept proposed herein, we estimate the crack locations for six scenarios with the trained ANN and compare the DLCs calculated for these locations with the DLCs calculated from the measured frequencies. The six scenarios used for testing the procedure are presented in Table 3. First, we present the natural frequencies obtained with the FEM in Table 3. The values are obtained from simulation, so we used up to four digits after the dot. This precision is achievable for the measured frequencies using proper excitation techniques [30] and signal processing algorithms [31]. However, based on its robustness, the damage detection method works even for fewer digits after the dot.

Afterward, we calculate the RFS values indicated in Table 4. Finally, we calculate the DLCs with equation (6); the results are presented in Table 5.

In Table 6, we present the crack locations which we found by involving the trained ANN. This table also presents the DLC values calculated for the identified positions.

Table 3. Natural frequencies obtained from simulation.

Scenario	x [m]	a [mm]	f_1 [Hz]	f_2 [Hz]	f_3 [Hz]	f_4 [Hz]	f_5 [Hz]	f_6 [Hz]	f_7 [Hz]	f_8 [Hz]
1	0.080	2	4.0406	25.477	71.5965	140.582	232.512	347.108	484.162	643.668
2	0.412	0.8	4.0883	25.607	71.7292	140.584	232.308	347.464	485.001	646.427
3	0.353	0.8	4.0876	25.615	71.7007	140.631	232.343	347.214	485.468	645.993
4	0.271	1	4.0846	25.623	71.6637	140.490	232.524	347.195	484.672	646.151
5	0.433	0.6	4.0859	25.5825	71.6884	140.536	232.007	347.461	484.431	646.0852
6	0.806	1.2	4.0899	25.6171	71.6374	140.253	232.006	347.201	485.475	646.032

Table 4. Relative frequency shifts calculated for the frequencies obtained by simulation.

Scenario	RFS_1	RFS_2	RFS_3	RFS_4	RFS_5	RFS_6	RFS_7	RFS_8
1	0.012067	0.005826	0.002235	0.000337	0.000078	0.001010	0.002694	0.004519
2	0.000415	0.000764	0.000386	0.000320	0.000951	-0.000014	0.000967	0.000252
3	0.000568	0.000457	0.000784	-0.000010	0.000802	0.000706	0.000004	0.000923
4	0.001320	0.000133	0.001300	0.000992	0.000023	0.000762	0.001643	0.000680
5	0.000984	0.001733	0.000955	0.000663	0.002247	-0.000005	0.002140	0.000781
6	0.000008	0.000387	0.001667	0.002681	0.002252	0.000748	-0.000011	0.000862

Table 5. Damage location coefficients calculated for the frequencies obtained by simulation.

Scenario	Generated x [m]	DLC_1	DLC_2	DLC_3	DLC_4	DLC_5	DLC_6	DLC_7	DLC_8
1	0.080	1	0.482836	0.18525	0.027963	0.006429	0.083721	0.223251	0.374476
2	0.412	0.428668	0.789809	0.399281	0.331424	0.983424	-0.01405	1	0.260166
3	0.353	0.615455	0.495218	0.849486	-0.01123	0.86905	0.765759	0.004589	1
4	0.271	0.803221	0.080754	0.791005	0.603812	0.014071	0.463708	1	0.413584
5	0.433	0.438045	0.771374	0.42508	0.295185	1	-0.00226	0.952361	0.347473
6	0.806	0.003106	0.14431	0.621672	1	0.840065	0.27893	-0.00406	0.321586

Table 6. Crack locations assessed via ANN and the resulting damage location coefficients.

Scenario	Assessed x [m]	DLC_1	DLC_2	DLC_3	DLC_4	DLC_5	DLC_6	DLC_7	DLC_8
1	0.0795	1	0.485707	0.183573	0.026841	0.006592	0.089073	0.229875	0.380552
2	0.3502	0.435600	0.798990	0.410484	0.329242	0.994951	0.000073	1	0.303938
3	0.2693	0.643461	0.517483	0.890846	0.004457	0.861860	0.848462	0.007845	1
4	0.4096	0.793785	0.086297	0.775438	0.614533	0.010720	0.447322	1	0.437225
5	0.3978	0.434971	0.691658	0.469599	0.195894	1	0.038255	0.764011	0.557471
6	0.8066	0.006416	0.145900	0.608157	1	0.849906	0.297893	0.000067	0.302231

The core of the procedure, which we propose in this paper, has to follow a standard damage detection method to check its accuracy. It compares the DLCs obtained from simulation/measurements (for the simulation, it is the generated location) with those obtained analytically for the identified crack position. So, knowing the DLCs for the actual (generated) locations induced in the FEM model and the identified locations obtained from the ANN, we can appreciate how these fit, thus, how correctly the crack location is estimated.

We use equation (7) to compare the DLC sets, which provide the Euclidian distance. In addition, we check the fit of the individual DLCs visually to observe differences between them. We present the results in Table 7 and in Figures 1 to 5. One can observe that not all simulated and estimated DLCs perfectly fit.

Table 7. DLC fit evaluation

Scenario	d_ε	Location x [m]		
		generated	assessed	difference
1	0.01103	0.080	0.0795	0.0005
2	0.05010	0.412	0.4096	0.0024
3	0.10069	0.353	0.3502	0.0028
4	0.03627	0.271	0.2693	0.0017
5	0.59358	0.433	0.3978	0.0352
6	0.03231	0.806	0.8066	-0.0006

From Table 7, we can observe that we did not estimate all crack locations with high accuracy. For instance, for scenario 5, the absolute error in estimating the position is 10.2 mm for the beam with a length of 1 m. The more significant error is signalized by the fit coefficient d_ε, which is significantly higher than for other scenarios.

A comparison of typical cases regarding the fit between the real DLCs and the DLCs for the estimated locations is represented in Figures 1 to 5. The closer the DLCs, the smaller the fit coefficient d_ε and the better the estimation of the crack location.

These visual representations in Figures 1 to 5 contribute to a better understanding of the results of the defect localization process. If the DLCs of the eight modes have, pair by pair, the same or very close amplitudes, the location is identified with high accuracy. This good fit is the case of Scenario 1 and Scenario 6, where the locations are assessed at 0.5 mm, respectively 0.6 mm from the generated location.

The location is not very accurately assessed if slight differences exist between the DLCs of several modes, such as those for Scenarios 2, 3, and 4. For these scenarios, absolute errors between 1.7 mm and 2.8 mm resulted.

Scenario 5 is an example of an inadequate assessment of the crack location. The significant differences between the generated and assessed DLCs indicate this fact. Indeed, we found an absolute error in estimating the crack location of 35.2 mm.

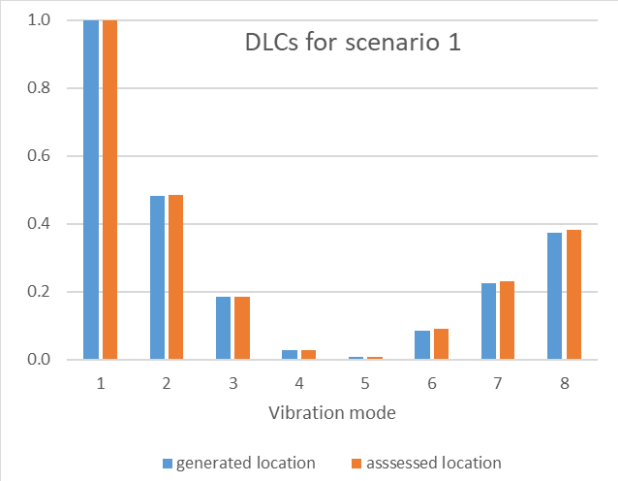

Figure 1. The DLC fit for an excellent location assessment – the case of scenario 1

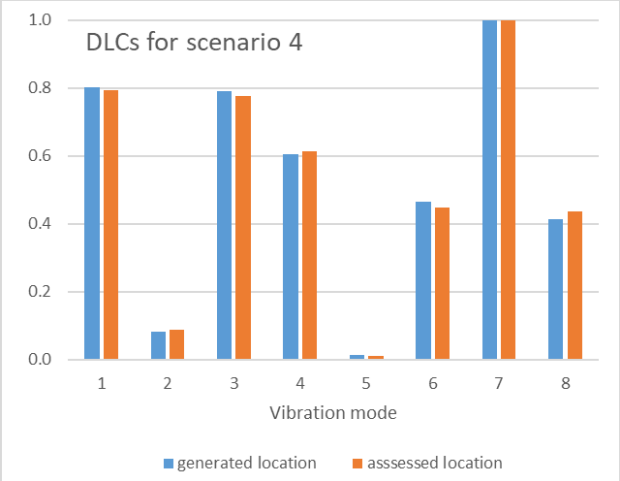

Figure 4. The DLC fit for an acceptable location assessment – the case of scenario 4

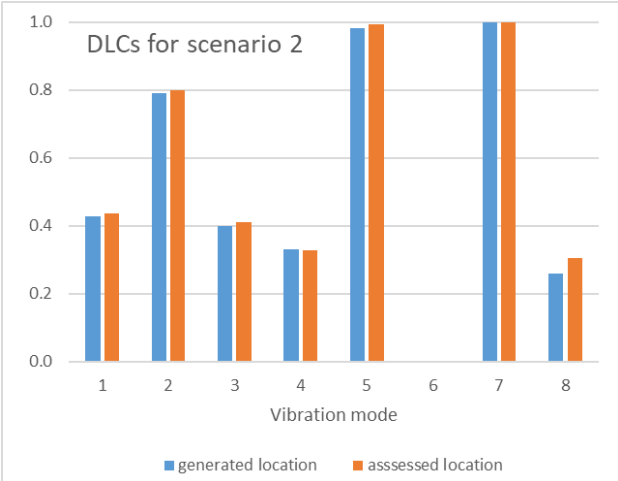

Figure 2. The DLC fit for an acceptable location assessment – the case of scenario 2

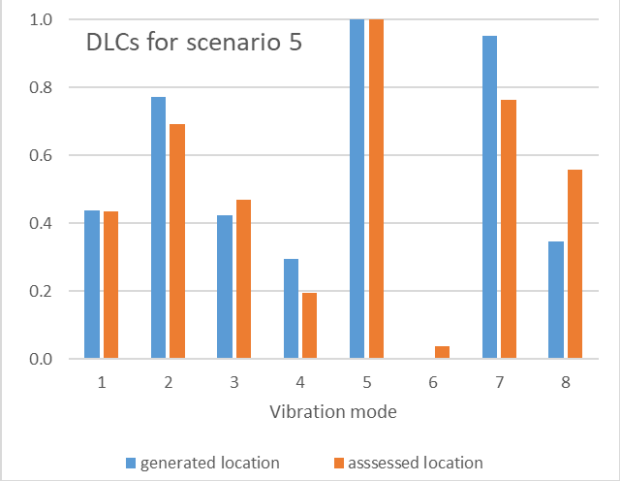

Figure 5. The DLC fit for an inadequate location assessment – the case of scenario 5

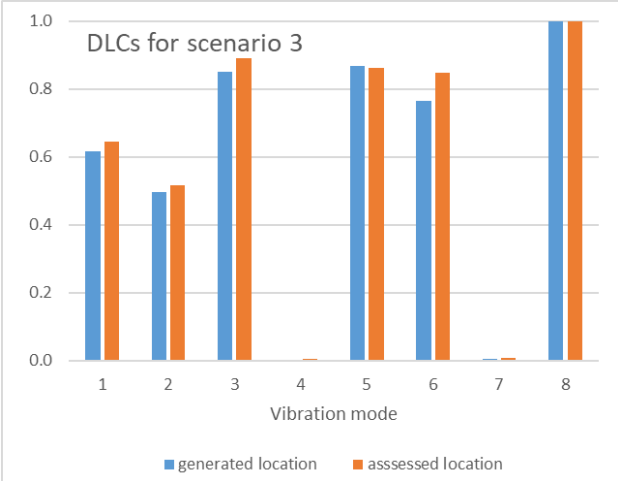

Figure 3. The DLC fit for an acceptable location assessment – the case of scenario 3

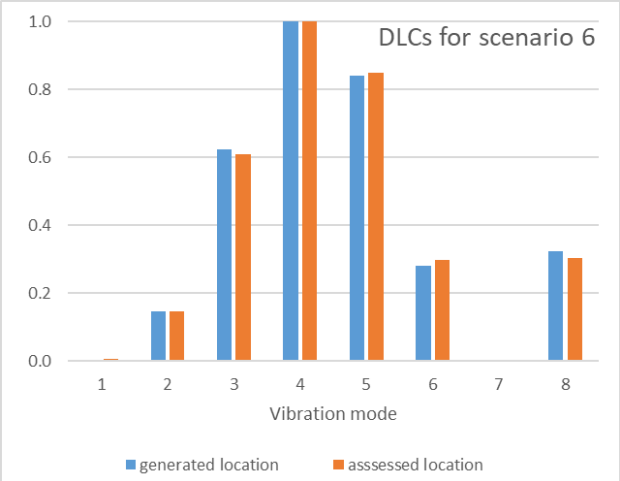

Figure 6. The DLC fit for an excellent location assessment – the case of scenario 6

We can observe that the DLCs obtained for the crack generated at location 0.412 m (Scenario 2) differ slightly from the DLCs obtained for the cracks generated at location 0.408 m (Scenario 5). This slight difference is expected since the two generated crack locations are very close. However, the ANN indicated the presumed location close enough to the generated one, and the proposed validation procedure confirms the small distance between the generated and identified crack location.

Note that, for exemplification, we used simulated data. These replaced measured data which are used in the case of damage assessment on real-world structures.

The accuracy estimation cannot be made without an additional check because the ANN model is complex and is not transparent. Thus, the decisions of the learning model are not transparent and do not permit interpretability [32]. For this reason, we added a tool for the end-users that gives them coherent explanations of the decisions and allow intervention when the automated decisions fail.

4. CONCLUSIONS

Artificial intelligence is generally used when large and complex data must be interpreted. One example is the vibration-based damage detection methods. Therefore, using ML techniques to assist damage detection methods is a common practice nowadays. The way the decisions are taken when ML is involved is not transparent, so humans must accept these decisions without proof of their reliability. However, the analysis results are sometimes unreliable, so explainability should be delivered simultaneously with the predictions. Alternatively, the system should automatically perform an assessment using another detection method or ML technique as a better solution than just informing about inaccuracies.

The main objective of this paper was to introduce a tool that permits checking the accuracy of damage detection predictions. The procedure compares the DLCs calculated using equation (5) for the location identified with the ANN model with the DLCs derived from the RFSs obtained via measurements.

We found out that:

- The accuracy of the damage detection method previously developed, which includes a simple ANN model, is satisfactory. The most significant absolute error we found after numerous experiments, indicated in this paper as Scenario 5, is 35.2 mm (3.52% of the beam length).
- The accuracy estimator, nominated as fit coefficient $\boldsymbol{d_{\varepsilon}}$, can predict if the crack location is identified correctly. We found that values less than 0.015 indicate an accurately predicted location, while values over 0.15 indicate a badly identified location.
- The diagrams representing the two DLC sets offer a suggestive image of the assessment accuracy.
- In all tests we performed, applying the proposed procedure, we could estimate correctly if the crack location were accurately found.

The accuracy estimation procedure we propose in this paper can be integrated with a standard damage assessment method so that the standard method is assisted by the first one and can avoid inaccurate predictions. For this reason, future concerns will consider integrating the proposed procedure with a standard vibration-based damage detection method. We will also focus on setting the limits of the fit coefficient to assess the error level more accurately and on assigning weights to the deviations of the vibration modes to obtain a more relevant fit coefficient.

As a shortcoming of the proposed procedure, we mention the need to know the effect of cracks on natural frequencies for a very dense network of locations on the structure. Getting this information is difficult for structures of high complexity.

REFERENCES

[1] Doebling S.W., Farrar C., Prime M.B., Shevitz D.W., A Review of Damage Identification Methods that Examine Changes in Dynamic Properties, *The Shock and Vibration Digest*, Vol.30, No.2, 1998.

[2] Salawu O.S., Detection of structural damage through changes in frequency: a review, *Engineering Structures*, Vol.19, No.9, 1997, pp. 718-723.

[3] Sinha J.K., Friswell M.I., Edwards S., Simplified models for the location of cracks in beam structures using measured vibration data, *Journal of Sound and Vibration,* Vol.251, No.1, 2002, pp. 13-38.

[4] Gillich G.R., Praisach, Z.I., Damage-patterns based method to locate discontinuities in beams, in: *Proc. SPIE 8695, Health Monitoring of Structural and Biological Systems 2013*, 869532, San Diego, USA, April 2013, 869532.

[5] Meriem S., Djamel N., Djilali B., Khatir S., Wahab M.A., Crack prediction in beam-like structure using ANN based on frequency analysis, *Frattura ed Integrità Strutturale*, Vol.59, 2022, pp. 18-34.

[6] Nguyen D.H., Abdel Wahab M., Damage detection in slab structures based on two-dimensional curvature mode shape method and Faster R-CNN, *Advances in Engineering Software*, Vol.176, 2023, 103371.

[7] Gillich G.R., Praisach Z.I., Onchis-Moaca D., Gillich N., How to correlate vibration measurements with FEM results to locate damages in beams, *Proceedings of the 4th WSEAS International Conference on Finite Differences - Finite Elements - Finite Volumes - Boundary Elements*, Paris, 2011.

[8] Rizos P.F., Aspragathos N., Dimarogonas A.D., Identification of crack location and magnitude in a cantilever beam from the vibration modes, *Journal of Sound and Vibration*, Vol.138, No.3, 1990, pp. 381–388.

[9] Imran M., Khan R., Badshah S., Experimental, analytical, and finite element vibration analyses of delaminated composite plates, *Transactions on Mechanical Engineering (B)*, Vol.28, No.1, 2021, pp. 231-240.

[10] Ciambella J., Pau A., Vestroni F., Modal curvature-based damage localization in weakly damaged continuous beams, *Mechanical Systems and Signal Processing*, Vol.121, 2019, pp. 171-182.

[11] Gillich G.R., Praisach Z.I., Iancu V., Furdui H., Negru I., Natural Frequency Changes due to Severe Corrosion in Metallic Structures, *Strojniški vestnik - Journal of Mechanical Engineering*, Vol.61, No.12, 2015, pp. 721-730.

[12] Imran M., Khan R., Badshah S., Investigating the Effect of Delamination Size, Stacking Sequences and Boundary Conditions on The Vibration Properties of Carbon Fiber Reinforced Polymer Composite, *Materials Research*, Vol.22, No.2, 2019, e20190478.
[13] Yang Z.B., Radzienski M., Kudela P., Ostachowicz W., Scale-wavenumber domain filtering method for curvature modal damage detection, *Composite Structures*, Vol.154, 2016, pp. 396-409.
[14] Minda P.F., Praisach Z.I., Gillich N., Minda A.A., Gillich G.R., On the efficiency of different dissimilarity estimators used in damage detection, *Romanian Journal of Acoustics and Vibration*, Vol.10, No.1, 2013, pp. 15-18.
[15] Seguini M., Khatir T., Khatir S., Boutchicha D., Djamel N., Wahab M.A., Crack Identification in Pipe Using Improved Artificial Neural Network. *In: Rao, R.V., Khatir, S., Cuong-Le, T. (eds) Recent Advances in Structural Health Monitoring and Engineering Structures. Lecture Notes in Mechanical Engineering*. Springer, Singapore, 2023.
[16] Khodabandehlou H., Pekcan G., Fadali M.S., Vibration-based structural condition assessment using convolution neural networks, *Structural Control and Health Monitoring*, Vol.26, No.2, 2018, e2308.
[17] Le H.Q., Truong T.T., Dinh-Cong D., Nguyen-Thoi T., A deep feedforward neural network for damage detection in functionally graded carbon nanotube-reinforced composite plates using modal kinetic energy, *Frontiers of Structural and Civil Engineering*, Vol.15, 2021, pp. 1453-1479.
[18] Wang Z., Cha Y.J., Unsupervised deep learning approach using a deep auto-encoder with an one-class support vector machine to detect structural damage, *Structural Health Monitoring*, Vol.20, No.1, 2020, pp. 406–425.
[19] Tran V.-T., Nguyen T.-K., Nguyen-Xuan H., Abdel Wahab M., Vibration and buckling optimization of functionally graded porous microplates using BCMO-ANN algorithm, *Thin-Walled Structures*, Vol.182, Part B, 2023, 110267.
[20] Dang B.-L., Nguyen-Xuan H., Abdel Wahab M., An effective approach for VARANS-VOF modelling interactions of wave and perforated breakwater using gradient boosting decision tree algorithm, *Ocean Engineering*, Vol.268, 2023, 113398.
[21] Ali R., Chuah J.H., Abu Talip M.S., Mokhtar N., Shoaib M.A., Structural crack detection using deep convolutional neural networks, *Automation in Construction*, Vol.133, 2022, 103989.
[22] Gillich N., Tufisi C., Sacarea C., Rusu C.V., Gillich G.R., Praisach Z.I., Ardeljan, M., Beam Damage Assessment Using Natural Frequency Shift and Machine Learning, *Sensors*, Vol.22, No.3, 2022, 1118.
[23] Gillich G.R., Maia N.M.M., Wahab M.A., Tufisi C., Korka Z.I., Gillich N., Pop M.V., Damage detection on a beam with multiple cracks: A simplified method based on relative frequency shifts, *Sensors*, Vol.21, No.15, 2021, 5215.
[24]. Praisach Z.I., Minda P.F., Gillich G.R., Minda A.A., Relative frequency shift curves fitting using FEM modal analyses, *Proceedings of the 4th WSEAS International Conference on Finite Differences - Finite Elements - Finite Volumes - Boundary Elements*, Paris, 2011.
[25] Gillich G.R., Praisach Z.I., Modal identification and damage detection in beam-like structures using the power spectrum and time-frequency analysis, *Signal Processing*, Vol.96, 2014, pp. 29-44.
[26] Kirmsher P.G., The effect of discontinuity on natural frequency of beams, in: *Proceedings of the American Society of Testing and Materials*, Vol.44, 1944, pp. 897-904.
[27] Chondros T.G., Dimarogonas A.D., Yao J., A continuous cracked beam vibration theory, *Journal of Sound and Vibration*, Vol.215, No.1, 1998, pp. 17-34.
[28] Tufisi C., Rusu C.V., Gillich N., Pop M.V., Hamat C.O., Sacarea C., Gillich G.R, Determining the Severity of Open and Closed Cracks Using the Strain Energy Loss and the Hill-Climbing Method, *Applied Sciences*, Vol.12, No.14, 2022, 7231.
[29] Gillich G.R., Aman A.T., Nedelcu D., Hamat C.O., Manescu T., Assessing multiple cracks in beams by a method based on the damage location coefficients, *Vibroengineering Procedia*, Vol.23, 2019, pp. 49-54.
[30] Mituletu I.C., Gillich G.R., Maia N.M.M., A method for an accurate estimation of natural frequencies using swept-sine acoustic excitation, *Mechanical Systems and Signal Processing*, Vol.116, 2019, pp. 693-709.
[31] Nedelcu D., Gillich G.R., A structural health monitoring Python code to detect small changes in frequencies, *Mechanical Systems and Signal Processing*, Vol.147, 2021, 107087.
[32] Le T.T.H., Prihatno A.T., Oktian Y.E., Kang H., Kim H., Exploring Local Explanation of Practical Industrial AI Applications: A Systematic Literature Review, *Applied Sciences*, Vol.13, No.9, 2023, 5809.